

Synthesis and Biological Activity of Tetrameric Ribitol Phosphate Fragments of *Staphylococcus aureus* Wall Teichoic Acid

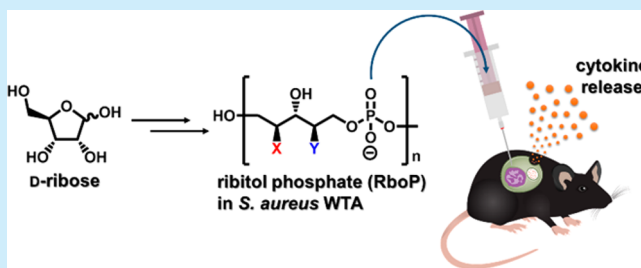
Yoon-Chul Jung,[†] Jae-Hyeok Lee,[†] Sang Ah Kim,[†] Timo Schmidt,[‡] Wonchul Lee,[†] Bok Luel Lee,^{*,‡} and Hee-Seung Lee^{*,†,§}

[†]Department of Chemistry, KAIST, Daejeon, 34141, Korea

[‡]National Research Laboratory of Defense Proteins, College of Pharmacy, Pusan National University, Busan, 46241, Korea

S Supporting Information

ABSTRACT: A systematically designed and synthesized ribitol phosphate (RboP) oligomer using a series of building blocks, which make up the wall teichoic acid (WTA) of *S. aureus*, is presented. Based on the use of a solution-phase phosphodiester synthesis, a library of ribitol phosphate tetramers, decorated with D-alanine and N-acetylglucosamine (GlcNAc), were generated. The synthesized RboP tetramers showed increased cytokine levels in mice in a subcutaneous air pouch model.



Infection by methicillin-resistant *Staphylococcus aureus* (MRSA) can cause fatal diseases such as endocarditis, osteomyelitis, sepsis, and other difficult-to-treat conditions.^{1–4} The absence of appropriate treatments against MRSA infections in terms of antibiotics and vaccinations has threatened public health and burdened healthcare systems worldwide. In low-income countries, the incidence of *S. aureus* disease is highest in neonates and children up to one year of age, and the mortality rates are estimated to be up to 50%. In the United States, *S. aureus* infection accounts for approximately 300,000 hospitalizations per year, and roughly 6% of those diagnosed with the disease lead to death.^{5,6} Since the emergence of MRSA, tremendous efforts have been devoted to develop a novel MRSA vaccine by both academia and pharmaceutical industries. However, to date no effective vaccine against MRSA has been brought to market.⁵

Over the past decade, several research groups have paid attention to wall teichoic acids (WTAs), glycopolymers displayed on Gram-positive bacterial peptidoglycan, as interesting molecules for a novel immune modulator. WTAs are known to control cell division, cell shape, and ion balance and behave as key virulence factors.⁷ Moreover, their importance in biofilm formation and antibiotic resistance is well studied.⁸ Upon an immune response, WTA is the target of the complement system (lectin ligand) and is recognized by the opsonophagocytic antibodies.⁹ These preliminary studies imply that WTA can serve as a valuable molecule to understand the molecular cross-talk between host and pathogen.¹⁰

WTA in *S. aureus* is connected to peptidoglycan in the bacterial cell wall by a phosphodiester bond, and it includes ribitol phosphate (RboP), glycerol phosphate (GroP), and ManNAc-GlcNAc disaccharides (Figure 1A).¹¹ RboP has a large role, accounting for more than 80% of WTA in molecular weight and is the outermost part of WTA. The chemical structure of

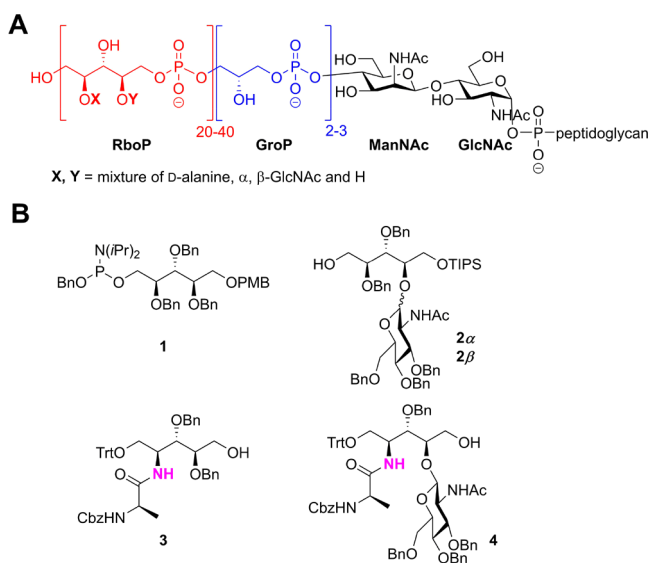


Figure 1. (A) Proposed chemical structure of wall teichoic acid (WTA) in *S. aureus*. Red: ribitol phosphate (RboP). Blue: glycerol phosphate (GroP). (B) Designed building blocks 1–4 for oligo RboP synthesis.

natural extracts of WTA from *S. aureus* shows three important features: (1) it is composed of 20–40 RboP units; (2) RboP contains GlcNAc with an α - or β -glycosidic linkage, and (3) D-alanine (Ala). Its lack of exact structural information due to its natural microheterogeneity and structural complexity of naturally sourced WTA hampers systematic analyses of host immune responses against *S. aureus* WTA. Thus, we envisioned

Received: June 2, 2018

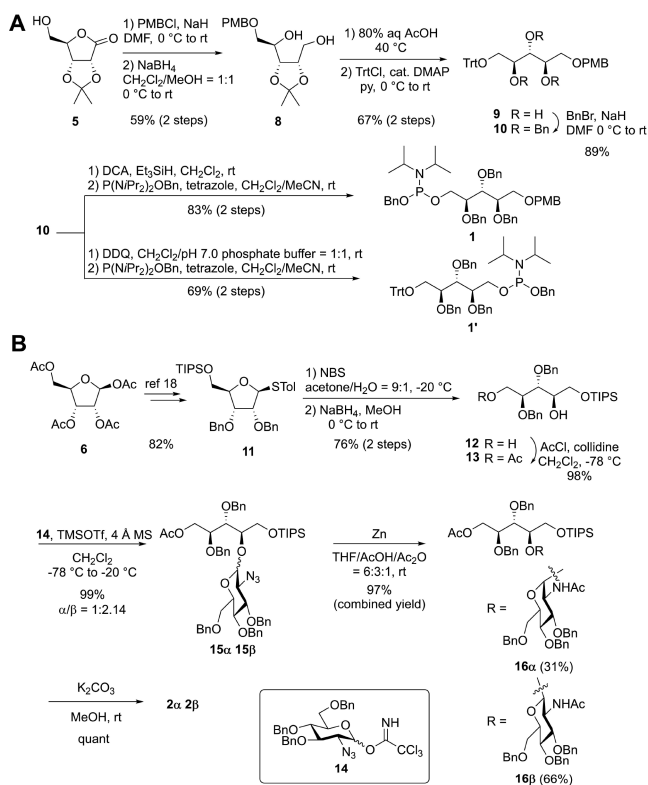
that various synthetic analogues of the oligo (RboP) in *S. aureus* with well-defined chemical structures would enable systematic and accurate analyses of host immune responses. Several groups have previously reported different synthetic strategies to access the well-defined glycerol phosphate based WTA and lipoteichoic acid (LTA) structures,¹² which include solution- and solid-phase synthesis, a fluorine-tagging strategy, and an enzyme-assisted semisynthetic approach. However, an RboP based WTA synthesis has rarely been exploited.¹³ Herein, we report the synthesis of ribitol phosphate of *S. aureus* derived WTA and its biological activity.

Our approach to synthesize RboP oligomers in *S. aureus* started with the design of its appropriate monomers and appendages, mainly GlcNAc and D-Ala (Figure 1B). Monomer 1 was designed for unmodified RboP, and all hydroxyl groups were fully protected with benzyl groups, except for two terminal hydroxyl groups. Monomer 2 has the appropriately protected form of GlcNAc substituents at the C4 hydroxyl group. In designing the D-Ala possessing building blocks 3 and 4, we hypothesized that the natural ester bond between the RboP oligomer and D-Ala could be cleaved undesirably in the synthetic process, and thus, we replaced the ester bond with a more stable amide bond in various reaction conditions. Although the amide functionality does not reflect naturally occurring RboP, previous results have shown the same biological activities when replacing ester with the amide D-Ala functional group in lipoteichoic acid (LTA).¹⁴ Monomer 4 consists of the D-Ala unit at the C2 nitrogen and a GlcNAc at the C4 oxygen. We envisioned that monomer 1 could be synthesized from the known D-ribonolactone derivative 5, monomer 2 from the commercially available 1,2,3,5-tetra-O-acetyl-D-ribofuranose 6, and monomers 3 and 4 from the known 2-deoxy-2-azido-ribo-1,4-lactone 7,¹⁵ respectively (Figure 1B).

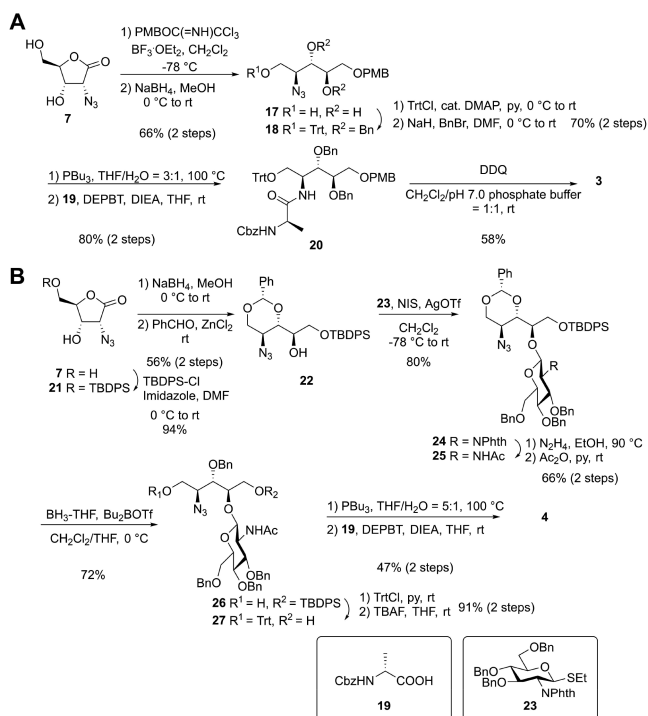
The construction of building blocks 1 and 2 is summarized in Scheme 1. The synthesis of building block 1 commenced with 2,3-isopropylidene-D-ribolactone 5.¹⁶ Protection of the hydroxyl group with *p*-methoxybenzyl (PMB) ether, followed by the reduction of the resulting lactone using NaBH₄, provided diol 8. Acidic hydrolysis of 8, followed by the treatment of the resulting triol with triphenylmethyl (Trityl) chloride, delivered triol 9 in 67% yield over two steps. Triol 9 was exposed to benzyl bromide in the presence of NaH to generate product 10. The removal of the Trityl group was achieved by using 10% dichloroacetic acid (DCA) in CH₂Cl₂ with triethylsilane as a cation scavenger, and the subsequent treatment of benzyl-oxybis(*N,N*-diisopropylamino)phosphine¹⁷ with 1*H*-tetrazole afforded the corresponding monomer 1. Similarly, monomer 1' was prepared in two steps from 10. Cleavage of PMB ether of 10, followed by the formation of phosphoramidite of the corresponding alcohol, provided monomer 1'.

The synthesis of building block 2 commenced with thioglycoside 11, which is readily prepared in four steps from the commercially available tetra-O-acetyl D-ribofuranose 6 at an 82% overall yield¹⁸ (Scheme 2B). Hydrolysis of thiotolyl with NBS, followed by the reduction of the resulting lactol using NaBH₄, provided diol 12. Next, diol 12 was treated with acetyl chloride and 2,4,6-collidine at -78 °C¹⁹ to yield glycosyl acceptor 13. Glycosylation of acetate 13 with trichloroacetimidate (TCA) glycosyl donor 14²⁰ in the presence of catalytic TMSOTf smoothly yielded a mixture of α - and β -glycosylate 15 α and 15 β , respectively. Satisfyingly, reductive amidation of mixture 15 α and 15 β with zinc in THF/AcOH/Ac₂O provided a separable mixture of acetamide 16 α and 16 β , which was

Scheme 1. Synthesis of Monomer 1 and 2



Scheme 2. Synthesis of Monomer 3 and 4



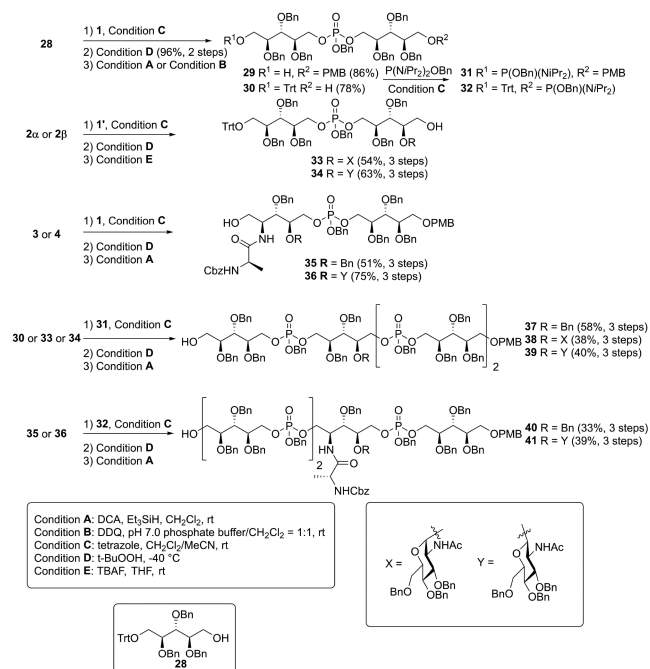
subjected to hydrolysis to form the monomers 2 α and 2 β with excellent yields.

Synthesis of building block 3 started from lactone 7 (Scheme 2). Exposure of lactone 7 to PMB-TCA with BF₃·OEt₂ in CH₂Cl₂, followed by NaBH₄ reduction, afforded triol 17 at a 66% yield over two steps. The subsequent protection of the primary alcohol to provide the trityl (Trt) ether was followed by

benzylation of the resulting diol to furnish **18**. The azide group at C2 was converted to an amine using the Staudinger protocol, followed by amide formation of the corresponding amine with amino acid **19** to give amide **20**. Finally, dissolving **20** in CH_2Cl_2 and pH 7.0 phosphate buffer (1:1) and the subsequent treatment with DDQ resulted in monomer **3**.

The synthesis of monomer **4** began with the formation of the TBDPS ether of lactone **7** to form product **21**. Reduction of **21** rendered the triol, which was converted to benzylidene acetal **22** in the presence of PhCHO and ZnCl_2 at a 56% yield over two steps. The glycosylation of glycosyl acceptor **22** with glycosyl donor **23**²¹ was promoted by NIS and AgOTf , leading to compound **24** at an 80% yield without formation of the α anomer. The *N*-phthalimido protecting group was then converted to a *N*-acetyl group using hydrazine, followed by treatment with acetic anhydride. Subsequently, the regioselective reductive cleavage of benzylidene acetal **24** was performed by treatment with $\text{BH}_3 \cdot \text{THF}$ and Bu_2BOTf to afford compound **25** at a 72% yield as the sole product. After protecting group manipulation (tritylation and desilylation), concomitant Staudinger reduction of the remaining azide resulted in the formation of an amine. Amide coupling with the resulting amine and **19** yielded monomer **4** at a 47% yield over two steps. With all four building blocks in hand, we focused on the oligomerization of our monomers to prepare tetramers **37**, **38**, **39**, **40**, and **41** (Scheme 3). Taking the precedent lipoteichoic

Scheme 3. Oligomerization of Monomers 1–4



acid (LTA) studies from Schmidt's group²² into account, we postulated that the tetramers are sufficient for studies on biological activities. First, we thought it would be possible to synthesize various oligomers by using a solid-phase nucleotide synthesizer (DNA synthesizer). However, too many monomers were consumed to make one oligomer at sufficient amounts for final deprotections and biological evaluations, which we deemed inefficient. Therefore, we turned our attention to a solution-phase synthesis. Phosphoramidite coupling of **1** and **28**²³ was achieved through activation with tetrazole, followed by an *in situ*

oxidation at -40°C with $t\text{-BuOOH}$ to form phosphate triester at a 96% yield. Detritylation of the corresponding triester afforded **29** in 86% yield and the removal of PMB group of triester afforded **30** at a 78% yield, which generated phosphoramidite **31** and **32**, respectively. To construct the dimer-containing GlcNAc subunit, the formation of a phosphate triester was attempted, followed by the treatment of TBAF, which resulted in $\alpha\text{-GlcNAc}$ **33** at a 54% yield and $\beta\text{-GlcNAc}$ **34** at a 63% yield over three steps, respectively. With the phosphate esters in hand, syntheses of tetramer **37**, **38**, and **39** were accomplished under the optimal conditions described above. Furthermore, we set out to prepare the tetramers containing the D-Ala functionality. Monomers **3** and **4** were subjected to phosphoramidite **1**, followed by oxidation and detritylation to yield the D-Ala dimers **35** and **36**. Both dimers **35** and **36** were coupled with phosphoramidite **32** to provide tetramer **40** at a 33% yield and **41** at a 39% yield after detritylation, respectively.

After global debenzoylation of the synthetic tetramers **37–41** (Figure 2A), to investigate the immunological activity of the

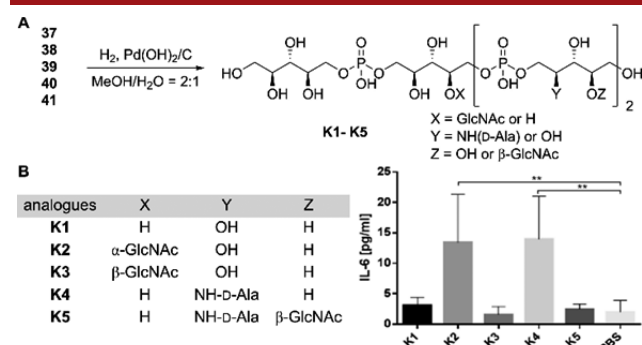


Figure 2. (A) Final global deprotection and tetramers which have modified functional groups. (B) Released cytokine IL-6 after the injection of 300 μg of the tetrameric ribitol phosphate fragments into a murine air pouch.

synthetic tetrameric RboP analogues, we performed cytokine release experiments using BALB/c mice. Subcutaneous air pouches were created in six-week old BALB/c mice, and then, the pouches were filled with 300 μg of the respective fragments **K1–K5** suspended in 1 mL of PBS buffer (the control group was injected with PBS only). After 5 h, the mice were sacrificed, and air pouches were washed with 1 mL of PBS. The supernatant from the air pouches was used to measure cytokine production with a cytometric bead array mouse inflammation kit. We found that the levels of interleukin-6 (IL-6), which is secreted by T-cells and macrophages to stimulate an immune response during an infection and acts as both a pro-inflammatory cytokine and an anti-inflammatory cytokine, had increased in response to the injected fragments **K2** and **K4** compared to the PBS injected negative control²⁴ (Figure 2B). Although the increment of the cytokine level was not profound, only the tetrameric RboP repeating units with $\alpha\text{-GlcNAc}$ and D-Ala functionalities could induce the immune response.

In conclusion, we systematically designed and synthesized a series of ribitol based monomers with or without GlcNAc and D-Ala functionalities from simple D-ribose derivatives with high efficiency and scalability, and each monomer was successfully oligomerized using phosphoramidite chemistry. The synthesized RboP tetramers increased the cytokine IL-6 level *in vivo* in the BALB/c air pouch model. As a first stage of this synthesis study, we showed relatively simple analogues of RboP tetramers

of the *S. aureus* WTA; however, we expect that these preliminary results will give further opportunities for investigations on immunological activities using the pure and chemically defined *S. aureus* RboP molecules. Moreover, due to the simplicity of the synthesis of the phospho-ribitol building blocks and oligomers presented here, plenty of different RboP analogues in terms of length, various combinations of extra substituents, and stereochemistry could be synthesized with precisely defined structures. With this established method, advanced immunological studies, such as cell recruitment and intradermal immunization studies for protection against MRSA infection, are currently ongoing. Those could pave the way to rationalize the use of MRSA immune modulators, such as vaccines, with high efficiency in the near future.

■ ASSOCIATED CONTENT

Supporting Information

The Supporting Information is available free of charge on the ACS Publications website at DOI: [10.1021/acs.orglett.8b01725](https://doi.org/10.1021/acs.orglett.8b01725).

Experimental procedures, characterization data, and NMR spectra (PDF)

■ AUTHOR INFORMATION

Corresponding Authors

*E-mail: hee-seung_lee@kaist.ac.kr.

*E-mail: brlee@pusan.ac.kr.

ORCID

Hee-Seung Lee: 0000-0003-0004-1884

Notes

The authors declare no competing financial interest.

■ ACKNOWLEDGMENTS

This research was supported by a National Research Foundation (NRF) of Korea grant funded by the Ministry of Science, ICT and Future Planning (2016R1A2A1A05005509). We thank Dr. Jintaek Gong (KAIST) for helping us to prepare the manuscript.

■ REFERENCES

- (1) Yoshikawa, T. T.; Bradley, S. F. *Clin. Infect. Dis.* **2002**, *34*, 211–216.
- (2) Lowy, F. D. N. *N. Engl. J. Med.* **1998**, *339*, 520–532.
- (3) Tong, S. Y. C.; Davis, J. S.; Eichenberger, E.; Holland, T. L.; Fowler, V. G., Jr. *Clin. Microbiol. Rev.* **2015**, *28*, 603–61.
- (4) Green, B. N.; Johnson, C. D.; Egan, J. T.; Rosenthal, M.; Griffith, E. A.; Evans, M. W. *J. Chiropr. Med.* **2012**, *11*, 64–76.
- (5) Giersing, B. K.; Dastgheyb, S. S.; Modjarrad, K.; Moorthy, V. *Vaccine* **2016**, *34*, 2962–2966.
- (6) Klevens, R. M.; Morrison, M. A.; Nadle, J.; Petit, S.; Gershman, K.; Ray, S.; Harrison, L. H.; Lynfield, R.; Dumyati, G.; Townes, J. M.; Craig, A. S.; Zell, E. R.; Fosheim, G. E.; McDougal, L. K.; Carey, R. B.; Fridkin, S. K. *JAMA* **2007**, *298*, 1763–1771.
- (7) (a) Neuhaus, F. C.; Baddiley, J. *Microbiol. Mol. Biol. Rev.* **2003**, *67*, 686–723. (b) Weidenmaier, C.; Peschel, A. *Nat. Rev. Microbiol.* **2008**, *6*, 276–287. (c) Brown, S.; Santa Maria, J. P., Jr.; Walker, S. *Annu. Rev. Microbiol.* **2013**, *67*, 313–336.
- (8) (a) Rockel, C.; Hartung, T. *Front. Pharmacol.* **2012**, *3*, 1–19. (b) Lynch, N. J.; Roscher, S.; Hartung, T.; Morath, S.; Matsushita, M.; Maennel, D. N.; Kuraya, M.; Fujita, T.; Schwaible, W. J. *J. Immunol.* **2004**, *172*, 1198–1202. (c) Brown, S.; Xia, G.; Luhachack, L. G.; Campbell, J.; Meredith, T. C.; Chen, C.; Winstel, V.; Gekeler, C.; Irazoqui, J. E.; Peschel, A.; Walker, S. *Proc. Natl. Acad. Sci. U. S. A.* **2012**, *109*, 18909–18914.
- (9) (a) Park, K. H.; Kurokawa, K.; Zheng, L.; Jung, D. J.; Tateishi, K.; Jin, J. O.; Ha, N. C.; Kang, H. J.; Matsushita, M.; Kwak, J. Y.; Takahashi, K.; Lee, B. L. *J. Biol. Chem.* **2010**, *285*, 27167–27175. (b) Jung, D. J.; An, J. H.; Kurokawa, K.; Jung, Y. C.; Kim, M. J.; Aoyagi, Y.; Matsushita, M.; Takahashi, S.; Lee, H. S.; Takahashi, K.; Lee, B. L. *J. Immunol.* **2012**, *189*, 4951–4959. (c) Kodali, S.; Vinogradov, E.; Lin, F.; Khoury, N.; Hao, L.; Pavliak, V.; Jones, C. H.; Laverde, D.; Huebner, J.; Jansen, K. U.; Anderson, A. S.; Donald, R. G. K. *J. Biol. Chem.* **2015**, *290*, 19512–19526.
- (10) (a) Sewell, E. W. C.; Brown, E. D. *J. Antibiot.* **2014**, *67*, 43–51. (b) Swoboda, J. G.; Meredith, T. C.; Campbell, J.; Brown, S.; Suzuki, T.; Bollenbach, T.; Malhowski, A. J.; Kishony, R.; Gilmore, M. S.; Walker, S. *ACS Chem. Biol.* **2009**, *4*, 875–883.
- (11) (a) Swoboda, J. G.; Campbell, J.; Meredith, T. C.; Walker, S. *ChemBioChem* **2010**, *11*, 35–45. (b) Brown, S.; Meredith, T.; Swoboda, J.; Walker, S. *Chem. Biol.* **2010**, *17*, 1101–1110.
- (12) For reviews, see: (a) van der Es, D.; Hogendorf, W. F. J.; Overkleeft, H. S.; van der Marel, G. A.; Codée, J. D. C. *Chem. Soc. Rev.* **2017**, *46*, 1464–1482. For solution- and solid-phase synthesis, see: (b) van Boeckel, C. A. A.; Visser, G. M.; Hermans, J. P. G.; van Boom, J. H. *Tetrahedron Lett.* **1981**, *22*, 4743–4746. (c) Hoogerhout, P.; Evenberg, D.; van Boeckel, C. A. A.; Poolman, J. T.; Beuvery, E. C.; van der Marel, G. A.; van Boom, J. H. *Tetrahedron Lett.* **1987**, *28*, 1553–1556. (d) Pedersen, C. M.; Figueroa-Perez, I.; Lindner, B.; Ulmer, A. J.; Zähringer, U.; Schmidt, R. R. *Angew. Chem., Int. Ed.* **2010**, *49*, 2585–2590. (e) Hogendorf, W. F. J.; Meeuwenoord, N.; Overkleeft, H. S.; Filippov, D. V.; Laverde, D.; Kropec, A.; Huebner, J.; van der Marel, G. A.; Codée, J. D. C. *Chem. Commun.* **2011**, *47*, 8961–8963. (f) Zhou, Z.; Ding, W.; Li, C.; Wu, Z. J. *Carbohydr. Chem.* **2017**, *36*, 205–219. For fluorine-tagging strategies, see: (g) Hogendorf, W. F. J.; Kropec, A.; Filippov, D. V.; Overkleeft, H. S.; Huebner, J.; van der Marel, G. A.; Codée, J. D. C. *Carbohydr. Res.* **2012**, *356*, 142–151. (h) Hogendorf, W. F. J.; Lameijer, L. N.; Beenakker, T. J. M.; Overkleeft, H. S.; Filippov, D. V.; Codée, J. D. C.; van der Marel, G. A. *Org. Lett.* **2012**, *14*, 848–851. (i) van der Es, D.; Berni, F.; Hogendorf, W. F. J.; Meeuwenoord, N.; Laverde, D.; van Diepen, A.; Overkleeft, H. S.; Filippov, D. V.; Hokke, C. H.; Huebner, J.; van der Marel, G. A.; Codée, J. D. C. *Chem. - Eur. J.* **2018**, *24*, 4014–4018. For semisynthetic approach, see: (j) Gale, R. T.; Sewell, E. D.; Garrett, T. A.; Brown, E. D. *Chem. Sci.* **2014**, *5*, 3823–3830.
- (13) Fekete, A.; Hoogerhout, P.; Zomer, G.; Kubler-Kielb, J.; Schneerson, R.; Robbins, J. B.; Pozsgay, V. *Carbohydr. Res.* **2006**, *341*, 2037.
- (14) Figueroa-Perez, I.; Stadelmaier, A.; Morath, S.; Hartung, T.; Schmidt, R. R. *Tetrahedron: Asymmetry* **2005**, *16*, 493–506.
- (15) Baird, P. D.; Dho, J. C.; Fleet, G. W. J.; Peach, J. M.; Prout, K.; Smith, P. W. J. *Chem. Soc., Perkin Trans. 1* **1987**, *1*, 1785–1791.
- (16) Tnay, Y. L.; Chiba, S. *Chem. - Asian J.* **2015**, *10*, 873–877.
- (17) Bannwarth, W.; Trzeciak, A. *Helv. Chim. Acta* **1987**, *70*, 175–186.
- (18) Kurosu, M.; Li, K. J. *Org. Chem.* **2008**, *73*, 9767–9770.
- (19) Ishihara, K.; Kurihara, H.; Yamamoto, H. *J. Org. Chem.* **1993**, *58*, 3791–3793.
- (20) Geiger, J.; Reddy, B. G.; Winterfeld, G. A.; Weber, R.; Przybylski, M.; Schmidt, R. R. *J. Org. Chem.* **2007**, *72*, 4367–4377.
- (21) Kerekgyarto, J.; Agoston, K.; Batta, G.; Kamerling, J. P.; Vliegthart, J. F. G. *Tetrahedron Lett.* **1998**, *39*, 7189–7192.
- (22) Figueroa-Perez, I.; Stadelmaier, A.; Deininger, S.; von Aulock, S.; Hartung, T.; Schmidt, R. R. *Carbohydr. Res.* **2006**, *341*, 2901–2911.
- (23) Compound **28** was prepared during the deprotection of 4-methoxybenzyl ether **10**. See [Scheme 1A](#).
- (24) For detailed experimental description, see [Supporting Information](#).